CONF-900704--4

UCRL- 102584
PREPRINT

A Numerical Study of Silane Combustion

J. A. Britten
J. Tong
C. K. Westbrook

This paper was prepared for submittal to the
Twenty-third International Symposium on
Combustion, University of Orleans, France
July 22-27, 1990

December 1989

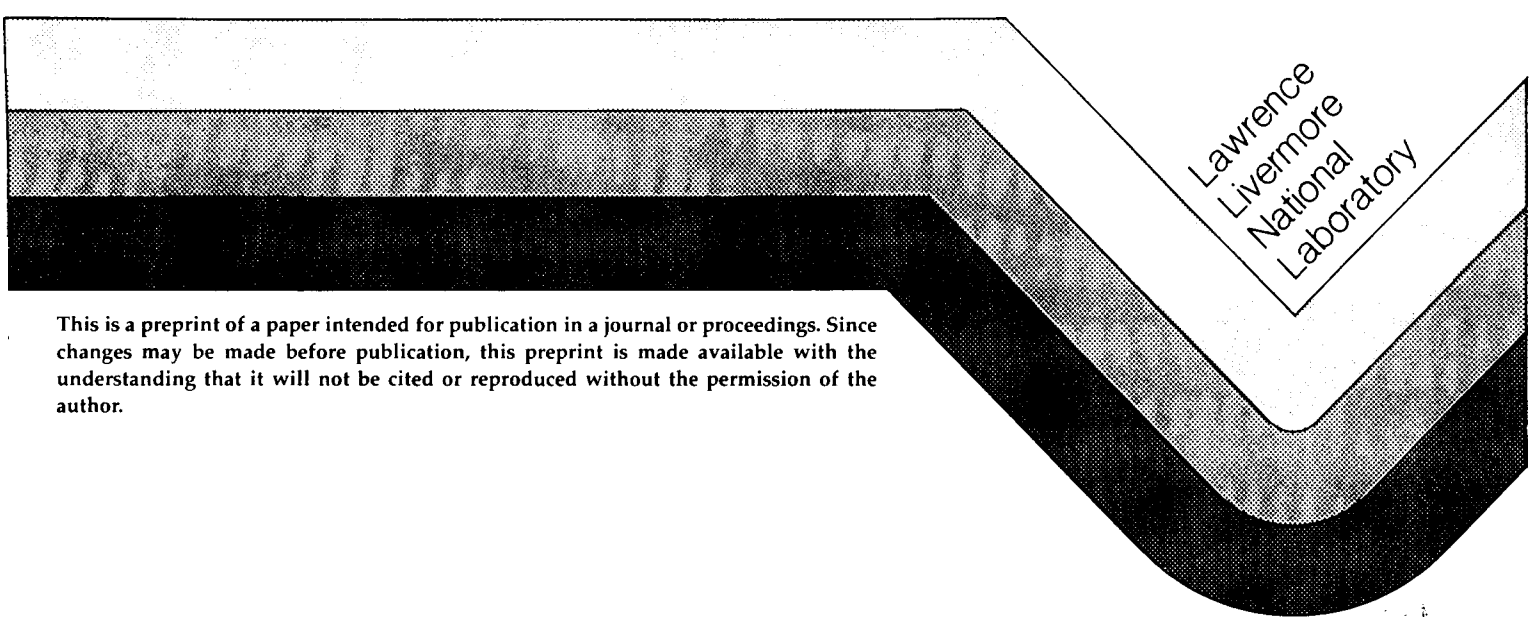

A NUMERICAL STUDY OF SILANE COMBUSTION

J. A. Britten, J. Tong[1] and C. K. Westbrook

Lawrence Livermore National Laboratory
Livermore, California 94550 U.S.A.

UCRL--102584

DE90 006002

A kinetic model of the mechanism of silane combustion has been developed, using a system of 70 elementary reaction steps and 25 chemical species. The model was used to examine silane ignition at ordinary pressures under both shock tube conditions and low-temperature constant-volume conditions. The agreement between model predictions and experimental data is very good, both with respect to shock tube ignition delay times and to the pronounced, nonlinear variation of autoignition time with initial pressure at near-ambient temperatures. The model also reproduces observed trends in H_2/H_2O product yield as a function of the initial SiH_4/O_2 ratio. One key to this mechanism is competition between thermal stabilization and chain-branching decomposition reactions of an excited-state silylperoxy radical, and a second key is the reaction of water vapor with intermediate species containing a Si=O double bond.

Introduction

An understanding of silane oxidation is important for many reasons. Deposition of SiO_2 insulating films by combustion of SiH_4 is a key process in the electronics industry[1,2]. Due to its pyrophoric nature, silane has been studied as an ignition promoter in supersonic jet engines[3–5], and silane is also used to ignite coal seams remotely during underground coal gasification[6,7]. It is due to this pyrophoricity that safety considerations for silane use in industrial applications provide perhaps the most compelling impetus for studying low-temperature silane-oxygen reactions.

The extreme reactivity and pressure sensitivity of silane-oxygen systems have long been known from experiment[8,9]. Little is known concerning the kinetic mechanism responsible for this behavior, however. This is in part due to the difficulty of characterizing the transitory intermediate species. It is generally agreed that the first step in silane oxidation is abstraction of an H atom from the parent SiH_4 by a radical species. Kinetic data for abstraction by H, OH and O radicals have been measured[10,11].

Silane decomposition has been extensively studied[12–14], and kinetic mechanisms

[1]presently at the University of California, Berkeley

for Si formation by silane pyrolysis, as well as thermodynamic data for intermediate species, have been established[15,16]. The key first step in silane decomposition is formation of silylene:

$$SiH_4 \rightarrow SiH_2 + H_2.$$

The SiH_2 intermediate is proposed to be very reactive toward oxidation, contributing to chain branching explosion. Silylene decomposition has been used along with reaction steps analogous to those of methane oxidation in a silane combustion mechanism proposed by Jachimowski and McLain[4]. These authors adjusted rate constants to obtain good agreement with shock tube ignition delay time data measured for silane-hydrogen-air systems at 800-1000 K[17].

In the present study, the mechanism of Jachimowski and McLain[4] was used initially to examine lower temperature (100-120 °C) autoignition of silane[8,18]. This mechanism failed to reproduce pyrophoric behavior at these conditions.

Recently, Hartman et al.,[18] have proposed a low-temperature silane oxidation mechanism involving a competition between thermal stabilization and chain-branching decomposition of a hot silylperoxy radical $SiH_3O_2\cdot$. This species is formed by addition of molecular oxygen to silyl (SiH_3) radicals produced by H atom abstractions from silane. The analogous addition of O_2 to methyl radicals to produce $CH_3O_2\cdot$ radicals is an essential part of the low-temperature reaction mechanisms for methane[19].

This paper reports on a numerical study of low-temperature silane oxidation in which chain propagation steps involving silylperoxy radicals, as suggested by Hartman et al., have been combined with reaction pathways similar to those of methane oxidation, as well as other pathways unique to this system. The mechanism studied here is far from a complete description of silane combustion. For example, nucleation of SiO_2 to form solid particulate has not been considered; this product is assumed to be created in its solid state by the elementary reactions. Also, combination or polymerization of Si-containing intermediate species has not been treated, and surface reactions probably important at lower pressures have not been considered. Finally, some thermochemical data for intermediate species have been only crudely estimated. Nevertheless, as will be shown below, this mechanism predicts quantitatively much of the available experimental data for silane-oxygen systems.

Numerical Model

Calculations were carried out with the HCT computer code[20], which solves the coupled conservation equations for mass, momentum, energy and chemical species in one dimension. Rate data for reactions comprising the mechanism are given in Table I. Rate constants for reactions of the hydrogen/oxygen subsystem have been

taken from an extensive base of thermochemical and rate data[21]. Some of the rate data for Si-reactions have been taken from the literature[4,10,11,15], and some estimated by comparison with analogous reactions in the chemistry data base characterizing methane oxidation. For these estimates, pre-exponential factors were left largely unchanged but activation energies for H-abstraction reactions were reduced to account for the weaker Si-H (≈90 kcal/mol) bond relative to C-H (≈105 kcal/mol).

Constants for the reverse reactions have been for the most part calculated from the forward rates and available or estimated thermochemical data. Thermochemical data used are given in Table II. Heat capacities for the Si-intermediates were assumed to be identical with those of C-analogs. Heats of formation for many of these species have been estimated by Hartman et al.,[18], and others have been estimated in the course of this work. Entropies of formation have been estimated[4], in the fashion illustrated by the following example:

$$S^o(HSiO) = S^o(SiO) + S^o(H) - \Delta S\ (HCO \rightarrow H + CO)$$

These values, along with enthalpies of formation have been used to estimate equilibrium constants of formation for use in calculating reverse rates. Where these calculations gave rise to unreasonable activation energies or pre-exponential factors, reasonable values were manually estimated.

The model developed was used to compute ignition delay times t_{ig} for a variety of mixtures of silane with oxygen and other constituents. All of the simulations assumed constant volume conditions, at temperature and pressure conditions corresponding to experiments with which the model results were to be compared. For some of the low-temperature simulations, a volumetric heat loss mechanism was incorporated into the model. Rate constants of key unmeasured reaction steps were adjusted to provide the best agreement between experimental and computed results, as discussed below.

Results

McLain et al.,[17] carried out shock tube experiments for mixtures of $SiH_4/H_2/O_2/N_2$, in which ignition delay times after passage of the reflected shock were determined. Calculations have been performed for these conditions, in which t_{ig} has been defined[4] as the time required for a temperature rise equal to 5% of the overall temperature rise experienced by the mixture. This is a somewhat arbitrary definition but is not felt to significantly influence the results due to the extremely rapid temperature rise experienced by the system. Results of the calculations are compared with the data for two conditions in Figure 1. The overall agreement between model and experiment is excellent, showing a well-defined Arrhenius dependence of t_{ig} on the initial temperature. The global activation energies for ignition under these conditions, calculated from the slope of the curves in Figure 1, are 22.4 and 23.8 kcal/mol.

Hartman et al.[18] discussed autoignition of silane/oxygen mixtures in constant volume reaction vessels and addressed particularly the upper-pressure explosion limits (the pressure above which a given mixture will not spontaneously explode) at low temperatures. Early studies had obtained conflicting data concerning the nature and extent of this pressure sensitivity, and Hartman et al., interpreted these results qualitatively in terms of a combination of kinetic factors, as well as effects of heterogeneous reactor wall contributions. The reaction mechanism proposed here provides a quantitative explanation for this behavior.

Figure 2 shows computed t_{ig} as a function of pressure for three temperatures, calculated for adiabatic conditions and a 70%/30% O_2/SiH_4 mix. Note the extremely rapid increase in t_{ig} with pressure over a very narrow pressure range, in particular at the lowest temperature. Inclusion of heat losses into the model calculations suppresses ignition of mixtures which exhibit long adiabatic t_{ig}, times, but has no effect on mixtures characterized by short adiabatic t_{ig}. For example, calculations were performed for a 70%/30% O_2/SiH_4 mix at 373 K using a heat loss coefficient of 20 W/m^2K, a value used in simulating ignition of hydrocarbon-air mixtures in Pyrex reactors[22]. Results showed that t_{ig} was unchanged from its adiabatic value of $2.1x10^{-3}$ s at 38.5 kPa, but at 43.5 kPa, $t_{ig} \approx 0.2$ s for the adiabatic case, heat losses completely suppressed ignition and the mixture temperature rise was less than 2 K after 60 s. The exact value of the pressure beyond which ignition is suppressed by heat losses and slow reaction occurs depends on the geometry and conditions of the experiment, but, given the steep dependence of t_{ig} on pressure evidenced in Figure 2, this limiting pressure should be quite well defined.

Lines of constant t_{ig}, again for a 70%/30% O_2/SiH_4 mix, are plotted on a pressure-temperature diagram along with data on explosion limits for 70/30 O_2/SiH_4 mixtures measured by experiment[18] in Figure 3. The individual symbols represent the experimental results for the pressure at which autoignition occurred, either as a result of pressure reduction of an initially stable mixture at a constant temperature, or temperature rise at a constant pressure. As such, time scales for ignition are not reported. With respect to the mechanism described here, it appears that the time scales for autoignition in the experiments of Hartman et al. were less than about 1 s. This provides a characteristic time for heat losses in their experiments somewhat less than 1 s, which is in agreement with other studies[22] and suggests that heat loss may play a role in the observed pressure sensitivity of SiH_4/O_2 systems.

Hartman et al. also measured yields of H_2 and H_2O in some experiments, and found that H_2O yields dominated for oxygen-rich systems while H_2 dominated for silane-rich systems. Product distribution was investigated with this model as a function of the initial silane/oxygen ratio at 40 kPa and 393 K, with heat loss and 50 % nitrogen dilution. This dilution was required for fuel-lean systems to overcome computational difficulties caused by extremely high calculated temperatures. Product yields were evaluated after the simulated system had cooled to ambient temperature, and were normalized by the number of moles of silane consumed in each case. These results are plotted in Figure 4, along with measurements of Hartman et al.,[18]

for pure silane/oxygen systems. The initial conditions of model and experiment are not identical, but the agreement in terms of the relative concentrations of H_2O and H_2 is striking.

Discussion

The key element in this mechanism, particularly with respect to low-temperature autoignition, is the competition between thermal stabilization and decomposition of the excited-state silylperoxy radical $xSiH_3O_2$ formed by reaction of SiH_3 and O_2:

$$SiH_3 + O_2 \longrightarrow xSiH_3O_2 \qquad \text{(R16)}$$
$$xSiH_3O_2 + M \longrightarrow SiH_3O_2 + M \quad \text{(stabilization)} \qquad \text{(R68)}$$

$$xSiH_3O_2 \longrightarrow SiH_3O + O \qquad \text{(R59)}$$
$$xSiH_3O_2 \longrightarrow SiH_2O + OH \qquad \text{(R60)}$$
$$xSiH_3O_2 \longrightarrow HSiOOH + H \qquad \text{(R61)}$$

The above is patterned largely after reaction steps proposed by Hartman, et al.,[18]. Rate constants for the above reactions are approximately the same as those calculated by these authors, although, in order to force quantitative agreement with all available data, reaction R60 has been assigned a temperature dependence with an activation energy of 6.3 kcal/mol. The stabilized radical SiH_3O_2 is allowed to decompose via reaction R36 with an activation energy of 40 kcal/mol[18].

Reaction R59 is crucial to this mechanism in that it creates a radical, O, which reacts with SiH_4 to create another radical OH. This provides the chain branching necessary for explosion. In fact, the steep increase in ignition delay time with pressure shown in Figure 2 occurs when the rate of the stabilization reaction R68 becomes comparable to R59, and thus the value of t_{ig} at low temperatures is extremely sensitive to the rate constants of these reactions. Given this extreme pressure sensitivity to chain branching and the demonstrated effect of heat losses, the model indicates that these combined effects can suppress autoignition at pressures above a critical pressure that depends on temperature and other condition. As a further illustration of the pressure sensitivity of silane/oxygen systems, it is of interest to note that use of silane to ignite coal underground is limited to relatively modest depths (less than about 200 meters, depending on the hydrostatic head)[6] since silane loses its pyrophoric properties at the higher pressures required to keep deeper seams dry.

For higher temperatures such as those of the shock tube experiments shown in Figure 1, chain branching provided by reaction R23 following silylene formation via reaction R26 begins to occur at rates comparable to that of reaction R59. Thus this reaction pathway influences ignition times as well.

Reaction R60 is the principal path for silylperoxy radical decomposition, even

though OH concentrations are somewhat less than H concentrations during the initiation stages of reaction. Calculations by Hartman et al.,[18] showed R60 to be the favored pathway for $xSiH_3O_2$ decomposition, However, these authors argued[18,23], on the basis of experimentally observed hydrogen/water product yields like those shown on Figure 4, that reaction R61 may be dominant since it involves hydrogen atoms and produces H_2, while the other reactions lead to water formation. The apparent inconsistency is resolved by inclusion of reactions R62, in which water is reduced by reaction with SiH_2O, and R63 in which SiH_2O reacts with OH to yield an H radical. This reaction scheme is based on the work of Kudo and Nagase[24] who have shown theoretically that the Si=O double bond in SiH_2O is unstable toward water or any polar molecule, and will react with no activation barrier. We have postulated that the silicon-containing species produced by these reactions is HSiOOH, which is also formed by direct decomposition of $xSiH_3O_2$ via R61. This species is therefore a major intermediate in our mechanism. This is consistent with identification of HSiOOH and H as intermediates in silane oxidation studies carried out by Niki et al.,[25].

Model calculations in which small concentrations of water vapor were included in the initial mixture showed that, provided reaction temperatures were sufficiently high, all of the water was reduced to H_2. This conflicts with experimental results of Hartman et al.,[18], who added small amounts of water to silane rich mixtures and found that some of this water survived the explosion. These authors used this evidence to further their postulate that silane explosions are driven mainly by H atoms. However, given the extreme reactivity of OH in H atom abstraction reactions of silane[11] leading to water formation, the preferential decomposition of $xSiH_3O_2$ to SiH_2O[18] and this species' reactivity toward toward water[24], it is reasonable to conclude that H_2O is formed and subsequently destroyed during silane/oxygen reactions. It may be that some water survived in the above-mentioned experiments by adsorbing on the reactor walls. Resolution of this question requires further study.

Removal of H from HSiOOH and its successor SiOOH completes the main reaction pathway to the SiO_2 product in this mechanism. During later stages of oxidation as H_2O and OH levels begin to decrease, production of HSiO from H atom abstraction of SiH_2O, mainly via R24, begins to become important. The HSiO then reacts to the final product SiO_2 via reactions R29-R35.

It appears that the H_2/H_2O product ratio is solely determined by thermodynamics. That is, the system is most stable when Si is fully oxidized, and provided the reaction temperature is sufficiently high Si will fully oxidize, and afterwards any excess oxygen will react with H_2 to form water. The preferential oxidation of silane in the presence of other fuels is also demonstrated in silane-methane/air counterflow diffusion flames, where CH_4 is merely a diluent in the silane flame[5]. Calculated H_2 yields for the most fuel-rich conditions in Figure 4 are less than thermodynamically predicted because temperatures in this low-heat release simulation were not high enough to fully convert the SiOOH intermediate. Also, much of the initial silane was left unreacted. Inclusion of a full set of silane pyrolysis reactions would provide

a pathway for silane pyrolysis to Si metal, and since pyrolysis is globally exothermic, it would facilitate the complete conversion of SiOOH also.

Calculations with this mechanism show that the ignition delay time for given pressure-temperature conditions decreases as the initial silane/oxygen ratio is increased. This is in agreement with the observations of Ring, et al.,[23] that silane-rich mixtures are more unstable than oxygen-rich ones.

Conclusions

A relatively detailed mechanism for silane combustion has been formulated and studied numerically, with the goals of quantitative agreement with experimental data on shock-tube ignition delay time and pressure sensitivity to autoignition at near-ambient temperatures. The mechanism developed achieves these goals, and also is capable of predicting H_2/H_2O product yield ratios for silane/oxygen explosions, and explaining the preferential oxidation of silane in multiple fuel mixtures under fuel-rich conditions. This mechanism appears promising, but requires further verification and refinement. The refinement includes modeling of product SiO_2 nucleation phenomena, intermediate species polymerization reactions, incorporation of silane pyrolysis reactions to predict product yields in silane-rich mixtures, and more accurate estimation of intermediate species thermochemical data.

Acknowledgement This work was performed under the auspices of the U.S. Department of Energy by Lawrence Livermore National Laboratory under contract number W-7405-Eng-48. Discussions with W.J. Pitz and computational support of L. Chase are greatly appreciated.

References

1. Strater, K.: *RCA Review* **29** 618 (1968)

2. Baliga, B.J., and Ghandi, S.K.: *J. Appl. Phys.* **44** 990 (1973)

3. Beach, H.L. Jr., Mackley, E.A., Rogers, R.C., and Chinitz, W.: 17^{th} JANAF Combustion Meeting, Vol. I., D.S. Eggleston, ed., CPIA Pub. 329, Appl. Phys. Lab., Johns Hopkins Univ., 639 (1980)

4. Jachimowski, C.J., and Mclain, A.G.: 'A Chemical Kinetic Mechanism for the Ignition of Silane/Hydrogen Mixtures' NASA TP 2129 (1983)

5. Northam, B.G., McLain, A.G., Pellet, G.L., and Diskin, G.: 'Effect of Silane Concentration on the Supersonic Combustion of a Silane/Methane Mixture' paper AIAA-86-1396, AIAA/ASME 22^{nd} Joint Propulsion Conference, Huntsville, Alabama, June 16-18, (1986)

6. Thorsness, C.B., Skinner, D.F., and Fields, D.B.: 'Laboratory Tests at Elevated Pressures of a Silane Igniter System for In Situ Coal Gasification' Lawrence Livermore Nat. Lab. rept. UCRL-53361 (1983)

7. Thorsness, C.B., Hill, R.W., and Britten, J.A.: Proc. 14^{th} Underground Coal Gasification Symposium, U.S. DOE rept. DOE/METC-88/6097 192 (1989)

8. Emeleus, H.J., and Stewart, K.: *J. Chem. Soc. (London)* 1182 (1935)

9. Schantarovitsch, P.S.: *Acta Physicochemica U.R.R.S.* **6** 65 (1937)

10. Austin, E.R., and Lampe, F.W.: *J. Phys. Chem.* **81**, 1134 (1977)

11. Atkinson, R., and Pitts, J. N.: *Int. J. Chem. Kinet.* **10** 1151 (1978)

12. Purnell, J.H. and Walsh, R.: *Proc. Roy. Soc. London* **A293** 543 (1966)

13. Newman, C.G., O'Neal, H.E., Ring, M.A., Leska, F., and Shipley, N.: *Int. J. Chem. Kinet.* **11** 1167 (1979)

14. Neudorfl, P., Jodhan, A., and Strausz, O.P.: *J. Phys. Chem.* **84** 338 (1980)

15. Coltrin, M.E., Kee, R.J. and Miller, J.A.: *J. Electrochem. Soc.* **131** 425 (1984)

16. Coltrin, M.E., Kee, R.J., and Miller, J.A.: *J. Electrochem. Soc.* **133** 1207 (1986)

17. McLain, A.G., Jachimowski, C.J., and Rogers., R.C.: 'Ignition of SiH_4-H_2-O_2-N_2 Behind Reflected Shock Waves' NASA TP-2114 (1983)

18. Hartman, J.R., Famil-Ghiriha, J., Ring, M.A., and O'Neal, H.E.: *Combust. Flame* **68** 43 (1987)

19. Benson, S.W.: '*Prog. Energy Combust. Sci.* **7** 125 (1981)

20. Lund, C.M.: 'HCT-A General Computer Program for Calculating Time-Dependent Phenomena Involving One-Dimensional Hydrodynamics, Transport, and Detailed Chemical Kinetics' Lawrence Livermore National Laboratory Report UCRL-52504 (1978)

21. Wilk, R.D., Cernansky, N.P., Pitz, W.J., and Westbrook, C.K.: *Combust. Flame* **77** 145 (1989)

22. Griffiths, J.F., Coppersthwaite, D., Phillips, C.H., Westbrook, C.K., and Pitz, W.J.: 'Auto-Ignition Temperatures of Binary Hydrocarbon Mixtures in a Closed Vessel: Comparisons Between Experimental Measurements and Numerical Predictions' *this Proceedings* (1990)

23. Ring, M.A., O'Neal, H.E., and Famil-Ghiriha, J.: Am. Inst. Physics Conf. Proc. #166, Photovoltaic Safety, Denver, Colorado, W. Luft, ed. (1988)

24. Kudo, T., and Nagase, S.: *J. Phys. Chem.* **88** 2833 (1984)

25. Niki, H., Maker, P.D., Savage, C.M., and Breitenbach, L.P.: *J. Phys. Chem.* **89**, 1752 (1985)

26. Pre-exponential factors taken from analogous C-reaction data of ref. 21, with activation energies reduced to reflect differences in bond energies.

27. Values ascribed in the course of this work.

List of Figures

TABLE I
Kinetic Constants for SiH_4 – O_2 Reaction Mechanism

no.	reaction	ref.	A_f^*	n_f	E_f	$A_r^\dagger$	n_r	E_r
R1	h2o + M = h+oh + M	21	2.20e+16	0.0	1.050e+05	1.400e+23	-2.0	0.
R2	ho2 + M = h+o2 + M	21	2.31e+15	0.0	4.590e+04	1.650e+15	0.0	-1.000e+03
R3	oh + M = o+h + M	21	8.00e+19	-1.0	1.037e+05	1.000e+16	0.0	0.
R4	o2 + M = o+o + M	21	5.10e+15	0.0	1.150e+05	4.700e+15	-0.3	0.
R5	h2 + M = h+h + M	21	2.20e+14	0.0	9.600e+04	3.000e+15	0.0	0.
R6	o2+h2 = oh+oh	21	8.00e+14	0.0	4.500e+04	2.760e+13	0.0	2.686e+04
R7	ho2+o = o2+oh	21	5.00e+13	0.0	1.000e+03	6.420e+13	0.0	5.661e+04
R8	h+o2 = o+oh	21	2.20e+14	0.0	1.679e+04	1.740e+13	0.0	6.770e+02
R9	h2+o = h+oh	21	1.80e+10	1.0	8.900e+03	8.300e+09	1.0	6.950e+03
R10	o+h2o = oh+oh	21	6.80e+13	0.0	1.835e+04	6.300e+12	0.0	1.100e+03
R11	h+h2o = oh+h2	21	9.50e+13	0.0	2.030e+04	2.200e+13	0.0	5.146e+03
R12	ho2 + M = o+oh + M	21	8.18e+21	-1.0	6.585e+04	1.000e+17	0.0	0.
R13	sih4+oh = sih3+h2o	11	8.70e+12	0.0	9.500e+01	5.028e+12	0.0	2.953e+04
R14	sih4+o = sih3+oh	11	4.00e+12	0.0	1.580e+03	2.345e+11	0.0	1.376e+04
R15	sih4+ho2 = sih3+h2o2	27	2.00e+12	0.0	1.000e+04	4.651e+11	0.0	6.234e+03
R16	xsih3o2 = sih3+o2	26	3.66e+20	-1.0	7.160e+04	3.000e+16	0.0	0.
R17	h+ho2 = oh+oh	21	2.50e+14	0.0	1.900e+03	1.200e+13	0.0	4.010e+04
R18	h+ho2 = h2+o2	21	2.50e+13	0.0	7.000e+02	5.500e+13	0.0	5.780e+04
R19	oh+ho2 = h2o+o2	21	5.00e+13	0.0	1.000e+03	6.330e+14	0.0	7.386e+04
R20	h2o2+o2 = ho2+ho2	21	4.00e+13	0.0	4.264e+04	1.000e+13	0.0	1.000e+03
R21	h2o2 + M = oh+oh + M	21	1.20e+17	0.0	4.550e+04	9.100e+14	0.0	-5.070e+03
R22	ho2+h2 = h2o2+h	21	7.30e+11	0.0	1.870e+04	1.700e+12	0.0	3.750e+03
R23	sih2+o2 = hsio + oh	4	1.00e+14	0.0	3.700e+03	7.066e+06	0.0	4.462e+04
R24	sih2o+h = hsio+h2	4	3.30e+14	0.0	1.050e+04	2.640e+12	0.0	2.517e+04
R25	sih2o+ho2 = hsio+h2o2	4	1.00e+12	0.0	8.000e+03	2.200e+10	0.0	6.593e+03
R26	sih4 = sih2+h2	15	5.00e+12	0.0	5.220e+04	7.109e+07	1.0	2.660e+03
R27	sih4 = sih3+h	15	3.69e+15	0.0	9.300e+04	2.612e+10	1.0	-1.600e+02
R28	hsio + M = h+sio + M	4	5.00e+14	0.0	2.900e+04	1.739e+11	1.0	1.156e+04
R29	hsio+h = sio+h2	4	2.00e+14	0.0	0.	1.311e+15	0.0	9.000e+04
R30	hsio+o = sio+oh	4	1.00e+14	0.0	0.	2.880e+14	0.0	8.790e+04
R31	hsio+oh = sio+h2o	4	1.00e+14	0.0	0.	2.839e+15	0.0	1.052e+05
R32	hsio+o2 = sio+ho2	4	3.00e+12	0.0	0.	5.271e+12	0.0	3.425e+04
R33	sio+o2 = sio2+o	4	1.00e+13	0.0	6.500e+03	0.	0.0	0.
R34	sio+oh = sio2+h	4	4.00e+12	0.0	5.700e+03	0.	0.0	0.
R35	sio2 + M = sio+o + M	4	0.	0.0	0.	2.500e+15	0.0	4.370e+03
R36	sih3o2 = sih2o+oh	26	8.60e+14	0.0	4.000e+04	0.	0.0	0.
R37	sih4+h = sih3+h2	10	1.50e+13	0.0	2.500e+03	2.002e+12	0.0	1.678e+04

TABLE I – Continued

R38	sih4+o2 = sih3+ho2	26	7.60e+13	0.0	4.40e+04	2.72e+12	0.0	2.54e+03
R39	sih2o+o = hsio+oh	4	1.80e+13	0.0	3.08e+03	1.75e+12	0.0	1.72e+04
R40	sih4+sih3o = sih3+sih3oh	26	2.00e+11	0.0	5.30e+03	1.05e+09	0.0	5.00e+04
R41	sih4+sih3o2 = sih3+sih3o2h	26	1.10e+13	0.0	1.85e+04	7.47e+11	0.0	6.09e+03
R42	sih3o2+sih2o = sih3o2h+hsio	26	1.30e+11	0.0	6.80e+03	2.50e+10	0.0	1.01e+04
R43	sih3o2+ho2 = sih3o2h+o2	26	4.00e+10	0.0	0.	3.0e+12	0.0	3.90e+04
R44	sih3o2h = sih3o+oh	26	6.50e+14	0.0	4.870e+04	2.5e+10	0.0	6.20e+04
R45	sih3o2h+h = sih3o2+h2	26	4.80e+13	0.0	7.950e+03	1.5e+14	0.0	1.60e+04
R46	sih3o+sih2o = sih3oh+hsio	26	1.20e+11	0.0	9.710e+02	5.2e+12	0.0	1.82e+04
R47	sih3o + sih3oh=sih3oh + sih2oh	26	1.50e+12	0.0	5.300e+03	2.80e+09	0.0	1.09e+04
R48	sih3o+o2 = sih2o+ho2	26	1.00e+12	0.0	4.50e+03	3.80e+13	0.0	3.22e+04
R49	sih3oh+h = sih2oh+h2	26	3.00e+13	0.0	5.30e+03	4.10e+11	0.0	1.30e+04
R50	sih3oh+o = sih2oh+oh	26	1.70e+12	0.0	1.73e+03	1.00e+10	0.0	7.80e+03
R51	sih3oh+oh = sih2oh+h2o	26	4.00e+12	0.0	1.50e+03	2.30e+11	0.0	2.50e+04
R52	sih3oh+sih3 = sih2oh+sih4	26	1.80e+11	0.0	7.40e+03	1.80e+10	0.0	1.30e+03
R53	sih3oh+sih3o2=sih2oh+sih3o2h	26	6.300e+12	0.0	1.450e+04	1.0e+09	0.0	1.00e+04
R54	sih3oh+o2 = sih2oh+ho2	26	4.00e+13	0.0	4.50e+04	1.90e+11	0.0	1.35e+03
R55	sih3oh+ho2 = sih2oh+h2o2	26	6.30e+12	0.0	1.40e+04	1.40e+11	0.0	4.10e+03
R56	sih2o+o2 = hsio+ho2	27	4.00e+14	0.0	2.95e+04	1.00e+14	0.0	3.00e+03
R57	sih2oh+o2 = hsiooh + oh	27	1.00e+13	0.0	7.00e+03	1.00e+15	0.0	1.20e+05
R58	hsio+sih3o = sio+sih3oh	27	1.00e+12	0.0	0.	6.00e+09	0.0	1.80e+04
R59	xsih3o2 = sih3o+o	27	1.76e+08	0.0	0.	0.	0.0	0.
R60	xsih3o2 = sih2o+oh	27	3.00e+12	0.0	6.33e+03	0.	0.0	0.
R61	xsih3o2 = hsiooh + h	27	1.14e+08	0.0	0.	0.	0.0	0.
R62	sih2o + h2o = hsiooh + h2	27	1.00e+13	0.0	0.	1.00e+12	0.0	4.00e+04
R63	sih2o + oh = hsiooh + h	27	1.00e+13	0.0	0.	1.00e+12	0.0	4.00e+04
R64	sih2o + ho2 = hsiooh + oh	27	1.00e+11	0.0	0.	0.	0.0	0.
R65	hsiooh + o2 = siooh + ho2	27	1.70e+13	0.0	1.60e+04	1.96e+10	0.0	4.98e+03
R66	hsiooh = siooh+h	27	5.00e+14	0.0	6.50e+04	1.00e+12	0.0	2.00e+04
R67	siooh+o2 = sio2+ho2	27	1.00e+12	0.0	1.43e+04	0.	0.0	0.
R68	xsih3o2 + M = sih3o2 + M	27	1.17e+13	0.0	0.	0.	0.0	0.
R69	siooh = sio2 + h	27	4.00e+15	0.0	8.4e+04	0.	0.0	0.
R70	siooh + h = sio2 + h2	27	1.00e+12	0.0	9.0e+03	0.	0.0	0.

* $_f$ forward rate

† $_r$ reverse rate

TABLE II

Heats of Formation and Equilibrium Constants of Formation $K_{eq} = A_{eq}e^{-E_{eq}/RT}$ for Silicon-Containing Species.

Species	ΔH_0^f Kcal/mol	A_{eq}	E_{eq} Kcal/mol
xsih3o2	-2.4200e+01		
sih3o	-2.2400e+01	5.95e+11	-2.16e+04
sih2o	-2.5280e+01	3.08e+12	-2.00e+04
sih2o2	-1.6500e+01	1.03e+00	-9.45e+04
hsiooh	-1.2470e+02	2.64e-10	-1.27e+05
siooh	-1.0900e+02	7.62e-05	-1.18e+05
sio2	-2.1574e+02	1.53	-7.30e+04
sih4	8.1980e+00	9.27e-12	9.16e+03
sih3	4.7790e+01	8.64e-08	4.86e+04
sih2	5.7990e+01	5.35e-05	5.87e+04
hsio	-4.8300e-01	1.41e+02	8.68e+03
sio	-2.4000e+01	2.68e+04	-2.76e+04
sih3o2h	-6.2100e+01	1.50e-09	4.62e+02
sih3oh	-7.4300e+01	1.60e-08	-4.96e+04
sih2oh	-3.2420e+01	1.86e+01	-4.07e+03
sih3o2	-2.4200e+01	6.60e-14	-5.88e+04

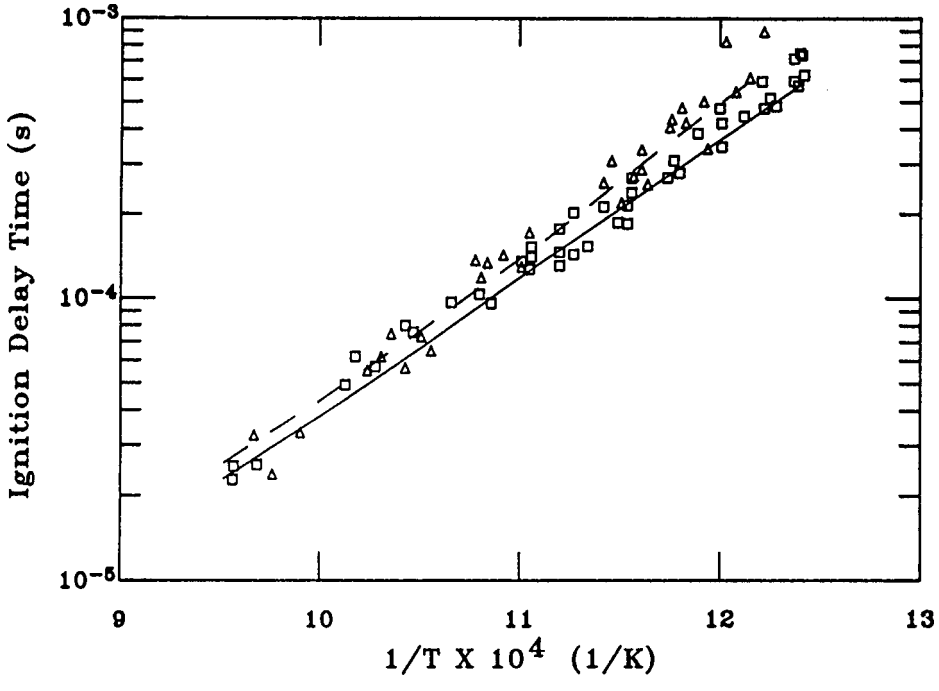

Figure 1 Calculated Shock-Tube Ignition Delay Times Compared with Experimental Data of ref. 17: Mixture of 2% SiH_4, 8% H_2, 4% O_2 and 86% N_2 at P = 126 kPa, □ – Measured, —— – Calculated; Mixture of 1.68% SiH_4, 6.72% H_2, 6.74% O_2 and 84.86% N_2 at P = 136 kPa, △ – Measured, — — – Calculated.

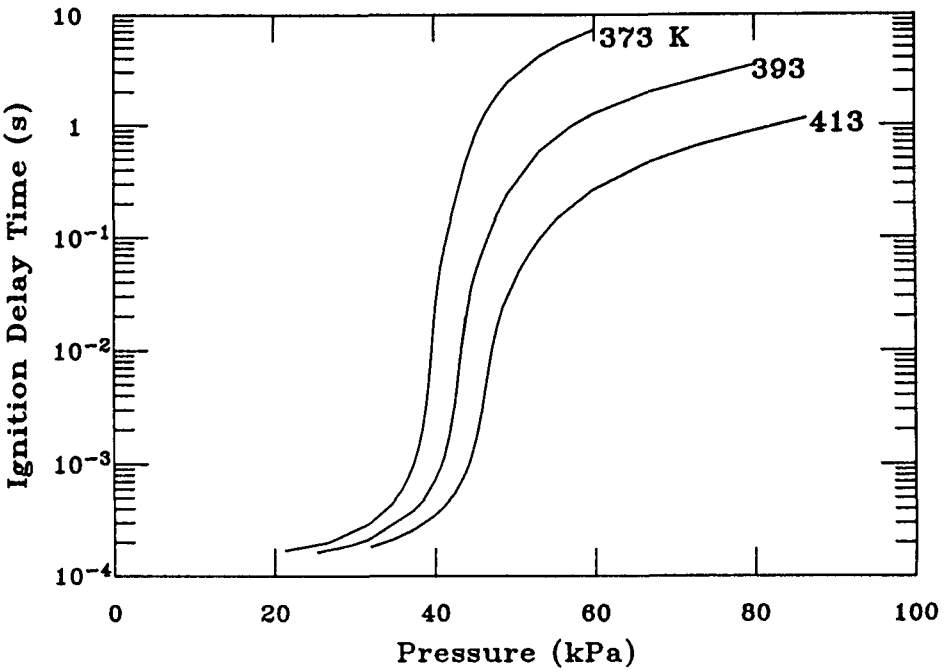

Figure 2 Calculated Adiabatic Ignition Delay Time as a Function of Pressure at Three Temperatures, for a 70%/30% Oxygen/Silane Mixture.

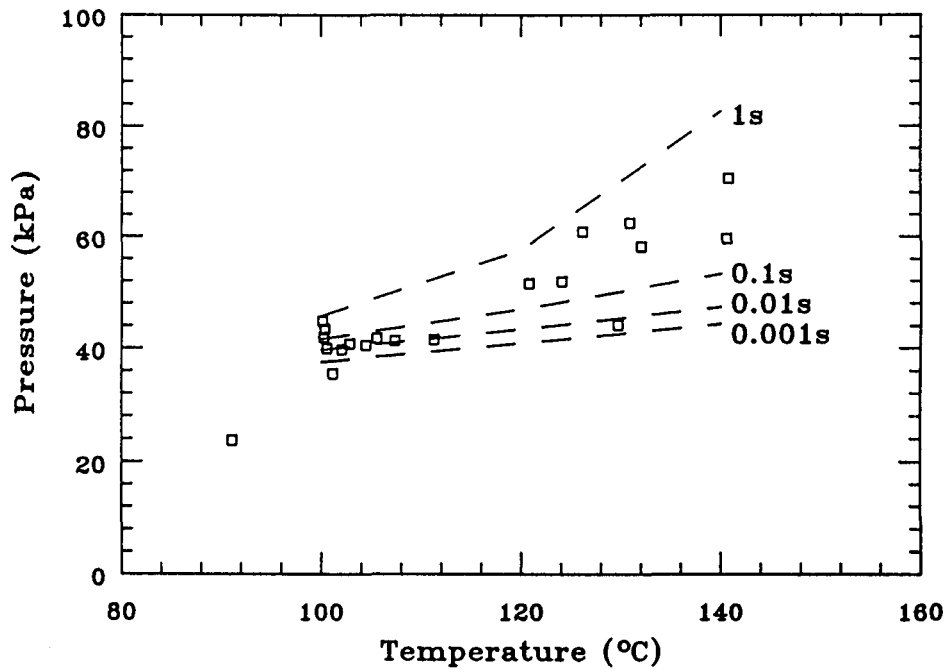

Figure 3 Lines of Constant Calculated Adiabatic Ignition Delay Time (— —) for a 70%/30% Oxygen/Silane Mixture, Plotted in Pressure-Temperature Space along with Explosion Limit Data of ref. 18 (□).

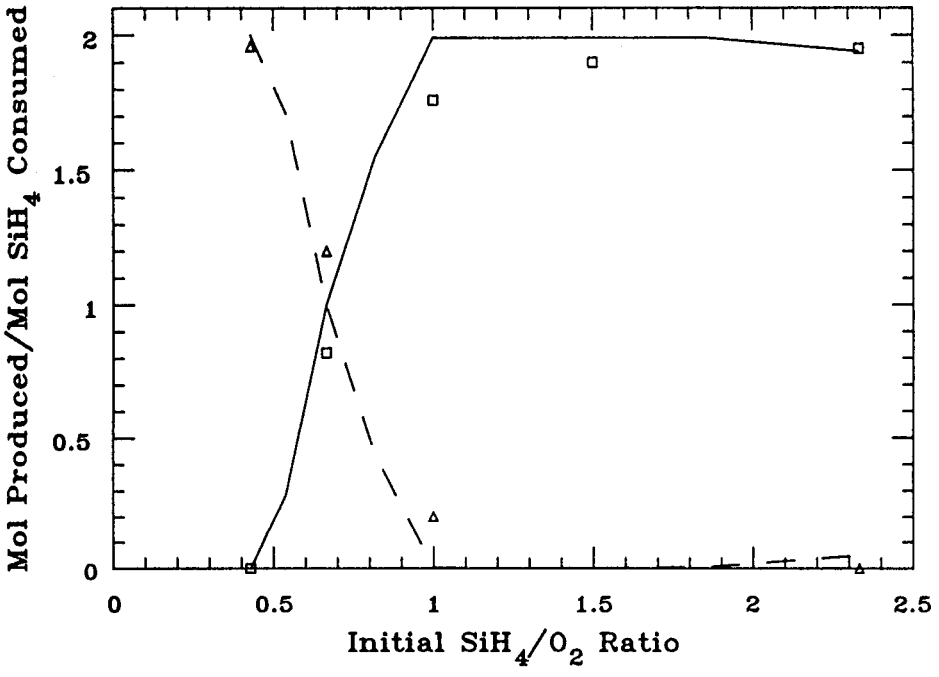

Figure 4 Calculated Ratios of H_2 and H_2O Produced per mole of SiH_4 reacted, plotted against initial SiH_4/O_2 Reactant Ratio, Compared with Experimental Data of ref. 18. —— H_2/SiH_4 (calculated); □ H_2/SiH_4 (measured); — — H_2O/SiH_4 (calculated); △ H_2O/SiH_4 (measured);

Technical Information Department · Lawrence Livermore National Laboratory
University of California · Livermore, California 94551